A study on local stresses of corrugated steel webs in PC bridges under prestressing

Shogo MORI[*], Takao MIYOSHI[**], Hisato KATOH[***]
Nobuo NISHIMURA[****], Satoshi NARA[*****]

Abstract

Generally, seldom corrugated steel webs in PC bridges do resist horizontal normal forces by prestressing and so on. However, bending deformation of the plates occurs at a point in the web plates far from connection between steel flanges and PC slabs. Normal stress caused by plate bending of the webs has influence on the durability of welded joint in steel girders. In this paper, at first, plate bending stress calculated by a practical equation is proposed. Proposed normal stress is verified by comparison with finite element analysis. Moreover, local stress distribution of the plates obtained by numerical analysis is discussed. As a result, a proposed practical equation is able to be applied in about middle 60% depth of the corrugated steel webs, and the plate bending stress in the vertical direction is even larger than in the horizontal one at the vicinity of connection between steel flanges and webs.

1 Introduction

PC bridge with corrugated steel webs, which replaces concrete webs of traditional PC box girder bridges by corrugated steel plates, is one of current structures. The bridge decreases total weight of the superstructure and cost of construction in comparison with traditional PC bridges. Moreover, advantage of using corrugated webs is to make shear buckling strength of the webs higher, prestressing works for PC slabs more efficient because of little horizontal stiffness, and to omit stiffeners in steel webs[1),2)]. In recent 10 years, these advantages promote construction of many PC bridges with corrugated steel webs in Japan. However, local stresses occurrimg in the corrugated web plates are not clarified.

Generally, bending moment causes uniform shear and vertical normal stresses in the corrugated steel webs near middle supports or loading point, due to negligible horizontal stiffness of the webs[1),2)]. However, the deformation of PC slabs by axial prestressing work or bend introduces plate bending deformation to corrugated steel webs. Therefore, it is important to evaluate plate bending stress of the webs, which is neglected in general design, because the stress has influence on the durability of welded joint in steel girders. It is not always practical to use experiments or finite element analysis (FEA) as a means of evaluating the local stress[3)]. This study aims at proposal of a simple equation which is effective for practical design work, and evaluation of the horizontal plate bending stress of the corrugated webs under prestressing.

In this paper, a simple equation to calculate the horizontal plate bending stress in corrugated webs is derived, and its verification and applicable range in vertical direction are shown using FEA. Also, the local stress distribution obtained by FEA is discussed.

* Graduate Student, Dept. of Civil Eng., Osaka University
** Dr. Eng., Designated Instructor, Dept. of Civil Eng., Osaka University
*** Dr. Eng., Manager, Bridge Engineering and Design Dept., JFE Engineering Corporation
**** Dr. Eng., Professor Emeritus, Osaka University
***** Dr. Eng., Professor, Dept. of Civil Eng., Osaka University

2 Proposed bending normal stress derived from a simple equation

The corrugated steel webs have symmetrically regular shape with a constant wave length in horizontal direction, as shown in Fig.2.1. To derive a simple equation, it is assumed that the plate with bending deformation is fixedly supported by PC slabs and flanges, and that axial deformation of the flanges is represented as the bending deformation of the webs on which a plane rahmen is modeled as shown in Fig.2.2.

Horizontal strain ε_c, which occurred in PC slabs due to prestressing, is given as follows,

$$\varepsilon_c = \frac{\sigma_{co}}{E_c} \qquad (2.1)$$

where, σ_{c0}: Magnitude of prestress introduced to PC slabs, and E_c: Elastic modulus of the concrete

If the axial deformation in each plate element of the corrugated web is negligible, the horizontal displacement ΔL occurring in a wavelength L of the corrugated web is caused by only rotation R of slant plate elements as shown in Fig.2.1. Then, ΔL is represented by the following equation,

$$\Delta L = 2c\{\cos(\alpha + R) - \cos\alpha\} \qquad (2.2)$$

As R is very small, it is possible to substitute relationships of $\cos R \fallingdotseq 1$ and $\sin R \fallingdotseq R$, for eq.(2.2), and, eq.(2.3) is obtained as follows,

$$\Delta L = -2cR\sin\alpha \qquad (2.3)$$

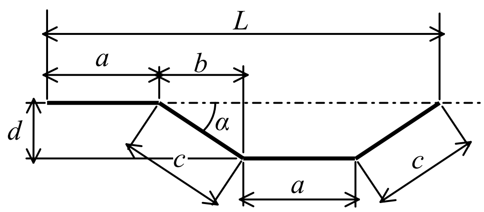

Fig.2.1 A wavelength of corrugated steel web

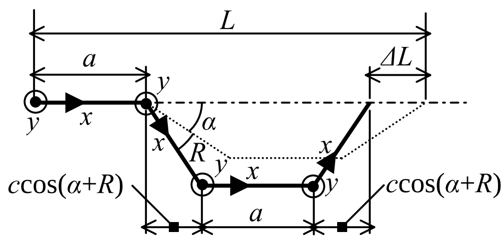

Fig.2.2 Deformation of corrugated steel web in axial direction

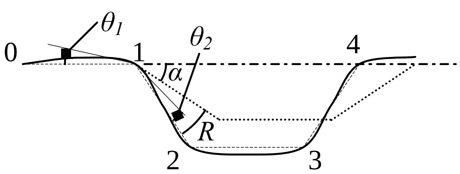

Fig.2.3 Plate bending deformation in a wavelength

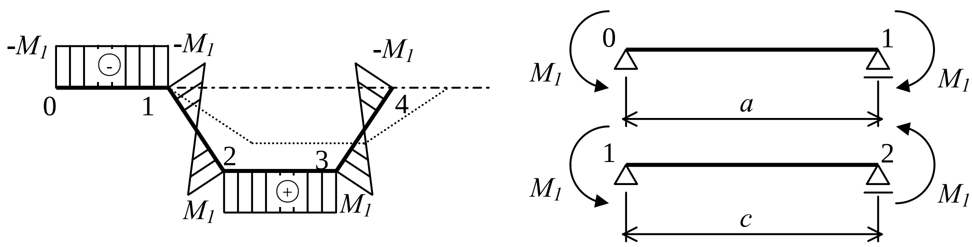

Fig.2.4 Distributions of plate bending moment

Using eq.(2.3), the apparent horizontal normal strain under prestressing is represented as follows.

$$\frac{\Delta L}{L}=\frac{-2cR\sin\alpha}{2(a+c\cos\alpha)}=-\frac{cR\sin\alpha}{a+c\cos\alpha} \tag{2.4}$$

From eq.(2.1) and (2.4), equation (2.5) is obtained by assumption that the plate bending deformation is not constrained by PC slabs and flanges.

$$R=-\frac{\sigma_{c0}}{E_c}\frac{a+c\cos\alpha}{c\sin\alpha} \tag{2.5}$$

As shown in Fig.2.3, compatibility condition of rotation at point-1 is represented as follows,

$$\theta_1=R-\theta_2 \tag{2.6}$$

Also, as shown in Fig.2.4, deflection angles θ_1 and θ_2 at point-1 and -2 are given, respectively, as follows,

$$\theta_1=\frac{M_1 a}{2EI} \tag{2.7}$$

$$\theta_2=\frac{M_1 c}{6EI} \tag{2.8}$$

where, E: Elastic modulus of a corrugated web, I: Moment of inertia of area, and M_1: Magnitude of the plate bending moment at point on folded line of a corrugated web.
Substituting eq.(2.7) and (2.8) to (2.6), R is represented as follows.

$$R=\frac{M_1}{EI}\left(\frac{a}{2}+\frac{c}{6}\right) \tag{2.9}$$

By substitution of eq (2.9) to (2.5), the plate bending moment M_1 is expressed by eq.(2.10).

$$M_1=-\frac{\sigma_{c0}}{E_c}\cdot\frac{EI(a+c\cos\alpha)}{3a+c}\cdot\frac{6}{c\sin\alpha} \tag{2.10}$$

Maximum absolute value of the plate bending stress occurs in both sides of a corrugated plate, and the simple equation is represented as follows using plate thickness t.

$$\sigma_p=\frac{M_1}{I}\cdot\frac{t}{2}=-\frac{\sigma_{c0}}{E_c}\cdot E\cdot\frac{1+\frac{c}{a}\cos\alpha}{1+\frac{c}{3a}}\cdot\frac{t}{c\sin\alpha} \tag{2.11}$$

Moreover, the stress calculated from eq.(2.11) is different from actual one as a thin walled structure, because eq.(2.11) is derived using assumption that a corrugated web is regarded as a plane rahmen.

The stress-strain relation for plane stress field is given as follows,

$$\begin{Bmatrix}\sigma_x\\ \sigma_y\\ \tau_{xy}\end{Bmatrix}=\begin{bmatrix}\frac{E}{1-\nu^2} & \frac{\nu E}{1-\nu^2} & 0\\ \frac{\nu E}{1-\nu^2} & \frac{E}{1-\nu^2} & 0\\ 0 & 0 & \frac{E}{2(1+\nu)}\end{bmatrix}\begin{Bmatrix}\varepsilon_x\\ \varepsilon_y\\ \gamma_{xy}\end{Bmatrix} \tag{2.12}$$

where, ν: Poisson's ratio of the corrugated web, and subscripts x and y of σ, τ, ε and γ are corresponded with the local coordinate system, as shown in Fig.2.2, respectively.
From eq.(2.12), when ε_y is much smaller than ε_x under prestressing, σ_x is evaluated approximately using the following equation.

$$\sigma_x = \frac{E}{1-\nu^2}\varepsilon_x \tag{2.13}$$

Also, from eq.(2.11), the simple equation to calculate the horizontal plate bending strain ε_p is represented as follows.

$$\varepsilon_p = -\frac{\sigma_{c0}}{E_c}\cdot\frac{1+\frac{c}{a}\cos\alpha}{1+\frac{c}{3a}}\cdot\frac{t}{c\sin\alpha} \tag{2.14}$$

By regarding ε_x in eq. (2.13) as ε_p in eq.(2.14), the simple equation to calculate the horizontal plate bending stress σ_{xb} is represented as follows.

$$\sigma_{xb} = \frac{M_1}{I}\cdot\frac{t}{2} = -\frac{\sigma_{c0}}{E_c}\cdot\frac{E}{1-\nu^2}\cdot\frac{1+\frac{c}{a}\cos\alpha}{1+\frac{c}{3a}}\cdot\frac{t}{c\sin\alpha} \tag{2.15}$$

3 Analytical models

In order to evaluate the bending normal stress σ_{xb} of the corrugated web represented by eq.(2.15), FEA is examined. Moreover, in order to clarify the applicable range of eq.(2.15), FEA models based on achievements of PC bridge with corrugated steel webs in Japan are set up. In this chapter, set up of analytical cases and models are shown.

3.1 Section parameters for models

Stress distributions in the corrugated web under prestressing are affected by the following factors; (1) height H_w, (2) thickness t, (3) folded angle α (see Fig.2.1), (4) dimensions a, b, c, and d (see Fig.2.1) of the web plate, (5) width and (6) thickness of the steel flange, (7) thickness and (8) (effective) length of the PC slab, and (9) a number of reinforcing bar in PC slabs. Stiffness of the corrugated web is affected by the parameters from (1) to (4), and constraint for plate bending deformation is dominated by the parameters from (5) to (9). It assumed that upper and lower flange are fixed to the PC slabs, and rigid against the out-of-plane deformation. Nine above parameters are determined in adequate ranges, based on achievements[3)] with regard to PC bridges with corrugated webs in Japan and the existing test specimen[6)] which is modeled on actual PC bridges with corrugated steel webs (90m in span length), as follows.

At first, H_w is equal to 1.2m, 1.5m, and 2.0m based on Fig.3.1 which shows relationship between maximum span length L_{max} and the averaged height of the web H_{wa}.

Secondly, frequency of α is high at 30deg. and 37deg. as shown in Fig.3.2. Therefore, α of the analytical model is set up 30, 36.87, and 53.13deg.

Finally, no-dimensional parameter t/H_w and H_w/a are defined using H_w which is determined from a specimen[6)], and a and t of this analytical model are set up from results of the linear regression analysis between t/H_w and H_w/a as shown in Fig.3.3.

Dimensions of the corrugated web, no. of wave in a span, name of analytical case and series are shown in Table 3.1 respectively. 4 analytical series, as shown in Table 3.1, have different parameters, a for Series-P1, α for Series-P2, t for Series-P3, and H_w for Series-P4, respectively.

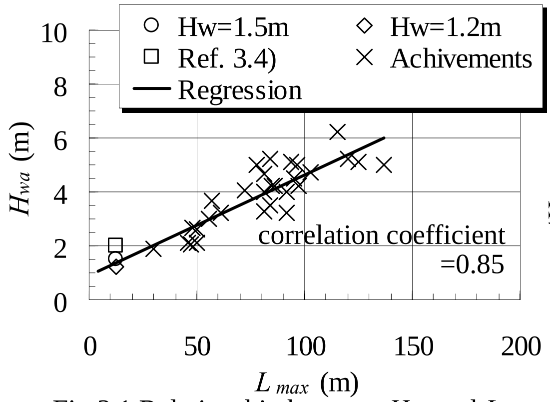

Fig.3.1 Relationship between H_{wa} and L_{max}

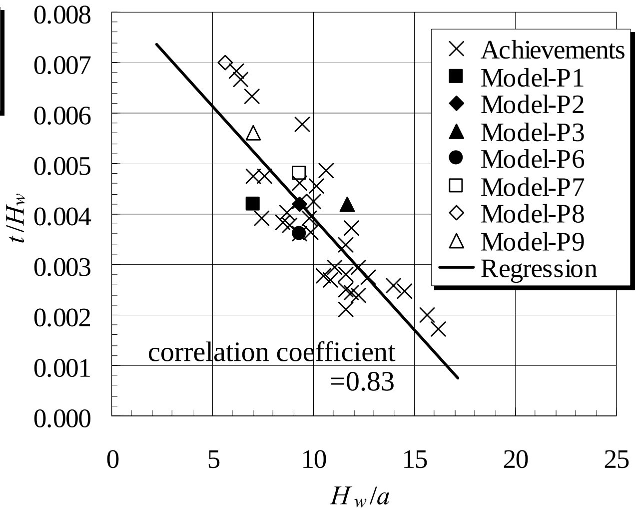

Fig.3.3 Relationship between t/H_w and H_w/a

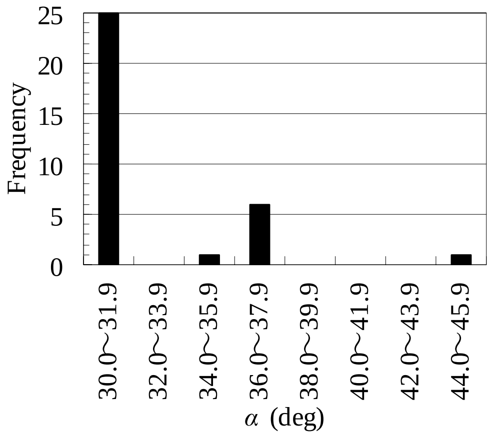

Fig.3.2 Histogram of bending angle in corrugated web plate

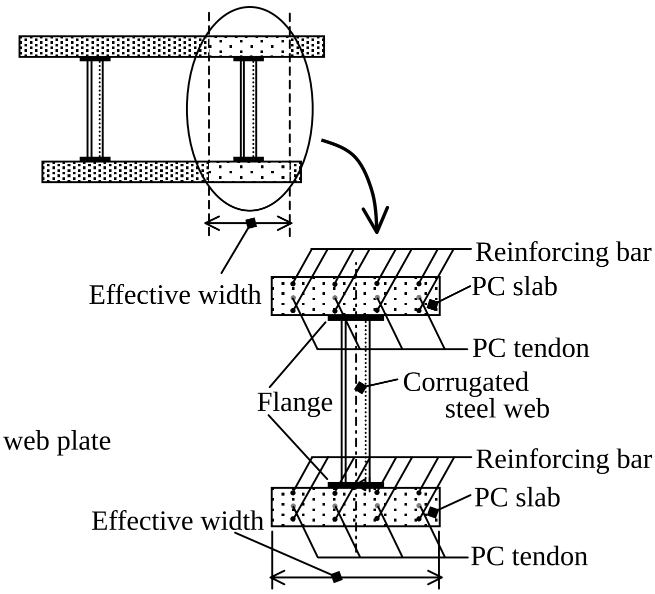

Fig.3.4 Cross-section of analytical model

3.2 Models for numerical analysis

As shown in Fig.3.4, in many existing research works[4)~7)] with regard to mainly behavior in vertical plane of PC bridges with corrugated steel webs, analytical models and specimens are modeled as a corrugated web and upper and lower PC slabs placed in one side. The simple equation (2.15) is derived from the model, shown by Fig.3.4. Analytical model for FEA is shown in Fig.3.5. Rigid connection between upper and lower flanges and PC slabs are postulated.

4 Results and discussion of numerical analysis

The plate bending stresses of the web obtained by FEA are discussed in comparison

Table 3.1 Dimensions of analytical models and analytical series for parametric analysis under prestressing

H_w (mm)	H_w/a	t/H_w	a (mm)	t (mm)	α (deg)	Wave length L (mm)	Span length L_s (mm)	No. of wave in a span	No. of analytical model	No. of analytical series
2000	6.9976	0.0042	286	8.4	30	1067	12800	12	Model-P1	Series-P1
	9.3301	0.0042	214	8.4	30	800	12800	16	Model-P2	
	11.6627	0.0042	171	8.4	30	640	12800	20	Model-P3	
2000	9.3301	0.0042	214	8.4	36.87	772	12347	16	Model-P4	Series-P2
	9.3301	0.0042	214	8.4	53.13	686	12347	18	Model-P5	
2000	9.3301	0.0036	214	7.2	30	800	12800	16	Model-P6	Series-P3
	9.3301	0.0042	214	8.4	30	800	12800	16	Model-P2	
	9.3301	0.0048	214	9.6	30	800	12800	16	Model-P7	
1200	5.5981	0.007	214	8.4	30	800	12800	16	Model-P8	Series-P4
1500	6.9976	0.0056	214	8.4	30	800	12800	16	Model-P9	
2000	9.3301	0.0042	214	8.4	30	800	12800	16	Model-P2	

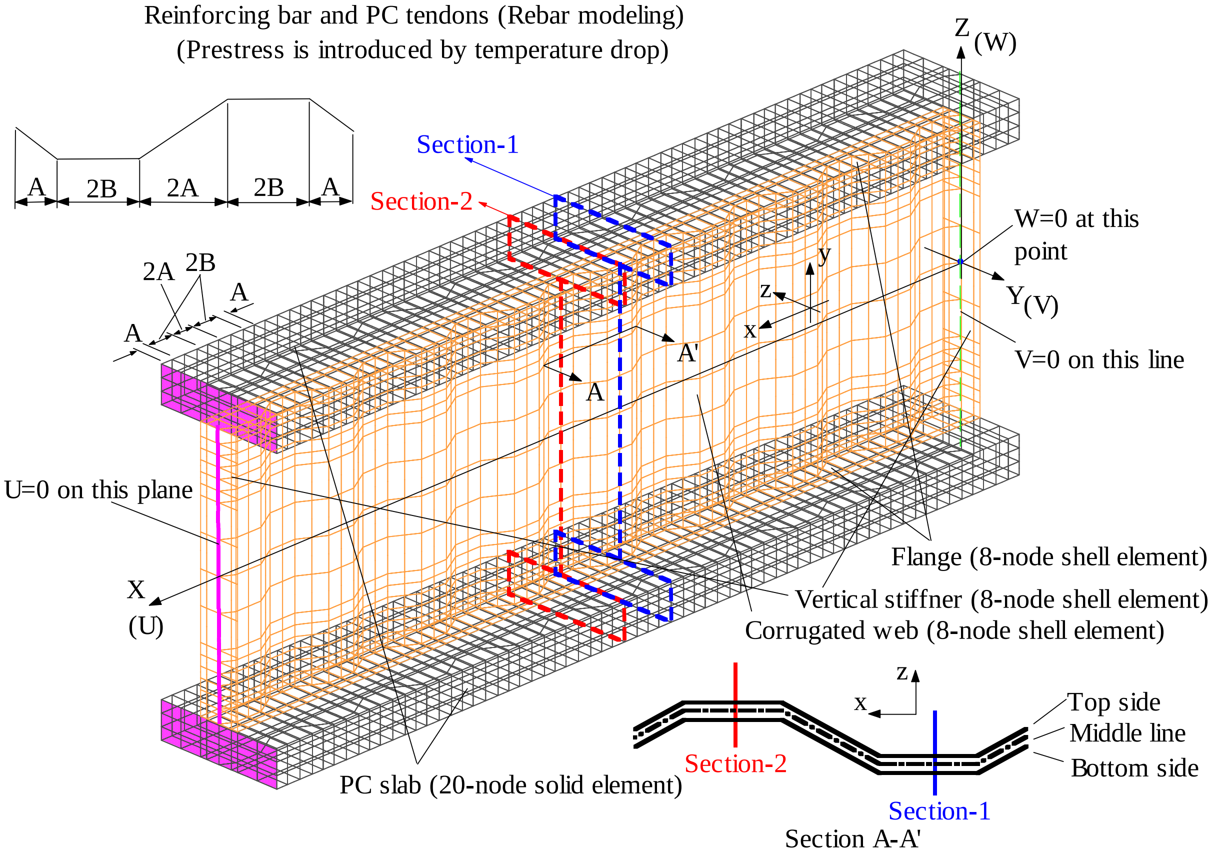

Fig.3.5 Analytical model under prestressing (Model-P2)

with those by the simple equation. Also, characteristic of the stress and strain distribution in the corrugated web is discussed, where location of cross-sections is focused at vicinity of 1/4-point in span length, because of negligible influence of load or boundary conditions on the behavior.

4.1 Characteristic of stress distribution

Figs.3.6 and 3.7 represent the stress distribution for the basic analytical model-P2 along vertical direction occurring at section-1 and 2 as shown in Fig.3.5 respectively. Local coordinate system (*x*-*y*-*z*) to describe stress component and two sides of the corrugated

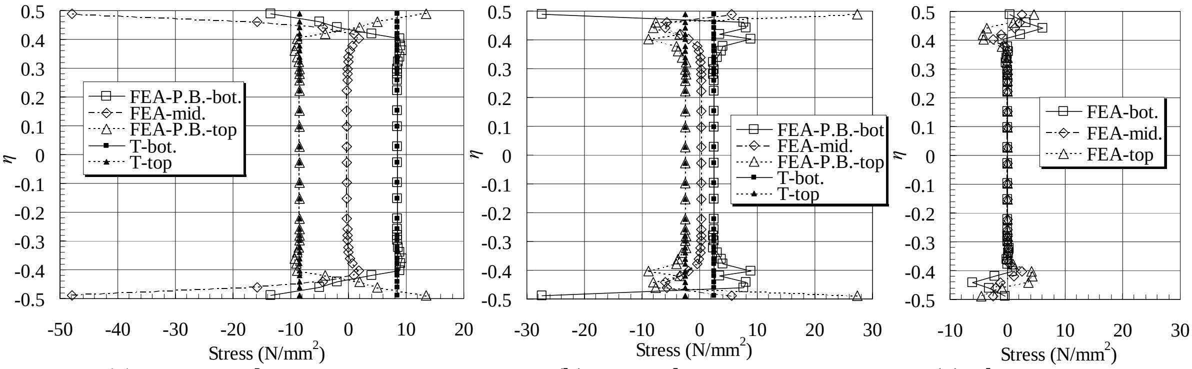

(a) Horizontal stress σ_x (b) Vertical stress σ_y (c) Shear stress τ_{xy}

Fig.3.6 Stress distributions at section-1 of Model-P2 along vertical direction

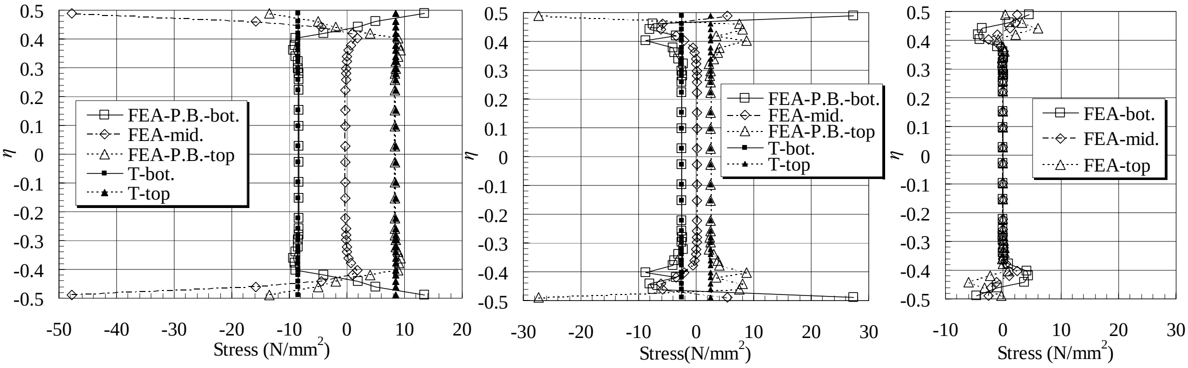

(a) Horizontal stress σ_x (b) Vertical stress σ_y (c) Shear stress τ_{xy}

Fig.3.7 Stress distributions at section-2 of model-P2 along vertical direction

plate are defined as shown in Fig.3.5. The stress component due to plate bending and membrane transformed from vertical and horizontal stress σ_x and σ_y are shown in Figs.3.6 and 3.7. "FEA" and "T" in their explanatory note represent the results of FEA and eq.(2.15), respectively. "P.B." represents the plate bending stress, and "bot.", "top", and "mid." in their explanatory note represent normal stresses occurring at bottom and top side of a corrugated plate, and mid-surface, respectively. Additionally, the vertical axis η in Figs.3.6 and 3.7 represents the normalized coordinate divided Z-coordinate in analytical models (see Fig.3.5) by height of the corrugated web H_w.

As shown in Figs.3.6(a) and 3.7(a), comparison between theoretical and FEA value of the horizontal bending stress shows that theoretical value get good agreement with FEA value in a range from η=-0.32 to η=+0.32. According to distributions of vertical plate bending stress as shown in Figs.3.6(b) and 3.7(b), plate elements parallel to bridge axis are subjected to constant bending stress around bridge axis in a range from η=-0.32 to η=+0.32. Figs.3.6(c) and 3.7(c) show that the in-plane shear stress τ_{xy} due to prestressing are almost negligible in a range from η=-0.38 to η=+0.38.

Figs.3.6 and 3.7 also show that the corrugated web is in bi-axial stress state constituted of the horizontal and vertical plate bending stress in the range from η=-0.32 to η=+0.32. However, the stress distribution close to the flanges varies immediately in the distance to the flanges. Careful investigation will be needed, because the stress component of vertical plate bending occurring at vicinity of connection portion between flanges and a

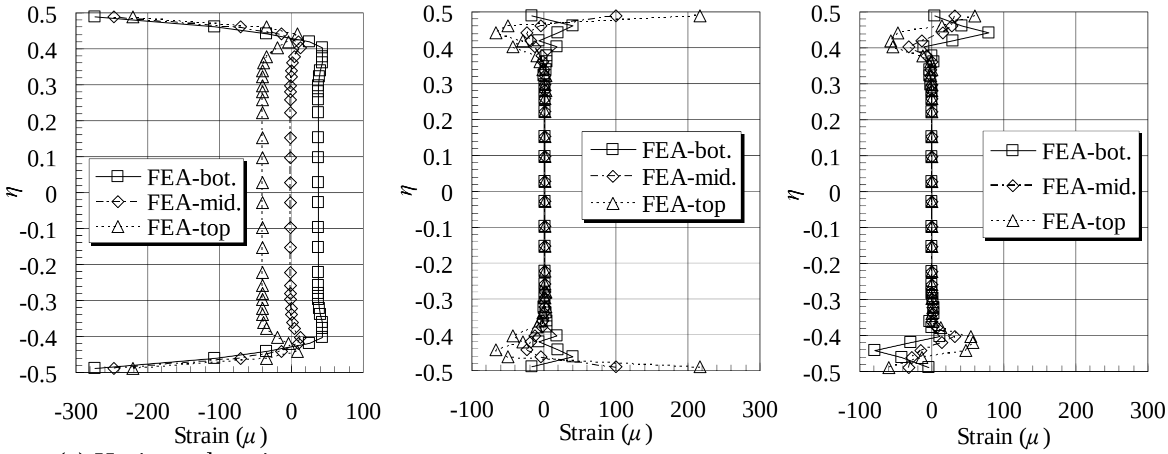

(a) Horizontal strain ε_x (b) Vertical strain ε_y (c) Shear strain γ_{xy}

Fig.3.8 Strain distributions at section-1 of model-P2 along vertical direction

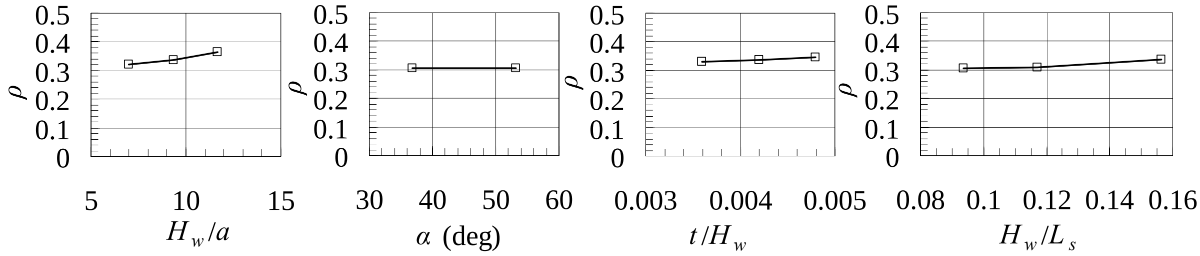

(a) Series-P1 (b) Series-P2 (c) Series-P3 (d) Series-P4

Fig.3.9 Changes of ρ for each analytical case under prestressing

corrugated web is about 6 times larger than that of vertical membrane, and the vertical plate bending stress is larger than horizontal one, in order to evaluate the durability of welded joints between a corrugated web and flanges.

4.2 Characteristic of strain distribution

As shown in Fig.3.8, each strain component represents constant distribution from η=-0.35 to η=+0.35, and each strain is concentrated in the area far from this range and located at vicinity of connection portion between flanges and a corrugated web. This trend is similar in the case of stress distribution. The vertical strain is almost zero in a range from η=-0.36 to η=+0.36. An assumption that ε_y is much smaller than ε_x under prestressing is appropriate shown by the figure. The vertical plate bending stress σ_{yb} is represented the following equation from eq.(2.12) and (2.14), using ε_y=0.

$$\sigma_{yb} = -\frac{\sigma_{c0}}{E_c} \cdot \frac{\nu E}{1-\nu^2} \cdot \frac{1+\dfrac{c}{a}\cos\alpha}{1+\dfrac{c}{3a}} \cdot \frac{t}{c\sin\alpha} \tag{4.1}$$

Distributions of σ_{yb} obtained by eq.(4.1) are shown in Figs.3.6(b) and 3.7(b) using "T" in their explanatory note. Theoretical and FEA value of σ_{yb} correspond well each other in a range from η=-0.32 to η=+0.32. Local deformation of the corrugated web in convex direction brings about a large σ_{yb}, occurring at vicinity of connection portion between flanges and a corrugated web.

4.3 Applicable range of the equation

Changes of ρ for each analytical series are shown in Fig.3.9. ρ denotes maximum value of no-dimensional coordinate η which represent the range held 5% in error is defined as an index in this research work. ρ is calculated as an averaged value at section-1 and 2 shown in Fig.3.5.

As shown in Fig.3.9(a), an applicable range of the simple equation is sensitive to the length of the plate element. Figs.3.9(b) and 3.9(c) show that folded angle and plate thickness of the corrugated web are independent on an applicable range which is constant from η=0.3 to η=0.35. Moreover, as shown in Fig.3.9(d), an applicable range of the simple equation is slightly affected by difference of the height of the corrugated web. Therefore, the equation is able to be applied in the range from η=0.3 to η=0.34.

5 Conclusions

In this research work, the simple equation to calculate the horizontal plate bending stress occurring in the corrugated web under prestressing is derived, and validity and the applicable range of the equation are investigated using FEA. Moreover, characteristic of local stress distribution occurring in a corrugated web is discussed. Achievements gained from this research work are as follows.

(1) Although the applicable range of the simple equation to calculate the horizontal plate bending stress varies slightly by changes of plate length parallel to bridge axis and height of the corrugated web, the range is from 30% to 34% up and down from central line of a corrugated web in vertical direction.

(2) Each in-plane stress occurring in a parallel plate element of the corrugated web to bridge axis under prestressing is distributed constantly at central portion of the corrugated web in vertical direction, and stress is in bi-axial stress state which is constituted of horizontal and vertical plate bending stresses.

(3) Each in-plane stress occurring at vicinity of connection portion between flanges and the corrugated web represents the concentration, because the corrugated web is locally deformed in convex direction and the bending deformation of plate elements is constrained elastically by upper and lower steel flanges.

(4) Careful investigations will be needed in order to evaluate the durability of welded joint at the connection portion, because the plate bending component of vertical stress occurring at vicinity of connection portion between flanges and a corrugated web represents about 6 times larger value than membrane component of that.

References

1) J. Combault (translated by T. Ohura) : The Maupre Viaduct near Charolees, France, Journal of Japan Concrete Engineering Association, Vol.34, No.1, pp.63-71, 1992. (in Japanese)
2) J. Combault, J.-D. Lebon and G. Pei : Box-Girders Using Corrugated Steel Webs and

Balanced Cantilever Construction, Proceedings of FIP Symposium ’93, Kyoto, Japan, pp.417-424, 1993.

3) Kinki branch of corporation of construction consultants : A Report to Construct the Performance-based Design Method for Steel and Composite Structures, 2004. (in Japanese)
4) K. Yamaguchi, T. Yamaguchi and S. Ikeda : Mechanical Behavior of Composite Prestressed Concrete Girders with Corrugated Steel Webs, Concrete Research and Technology, Vol.8, No.1, pp.27-40, 1997. (in Japanese)
5) K. Uehira, F. Yanagishita, T. Ebina and K. Sonoda : Experimental Study for Joint Methods of the Corrugated Steel Web of PC Box Girder, Concrete Research and Technology, Vol.9, No.2, pp.9-17, 1998. (in Japanese)
6) Y. Ata, M. Ochiai, Y. Mizoe and F. Machida : A Static and Fatigue Test with Full Scale Models for PC Box Girder Bridge Using Corrugated Steel Webs, Journal of Prestressed Concrete, Japan, Vol.43, No.4, pp.72-81, 2001. (in Japanese)
7) H. Shiratani, H. Ikeda, Y. Imai and K. Kano : Flexural and Shear Behavior of Composite Bridge Girder with Corrugated Steel Webs around Middle Support, Journal of Structural and Earthquake Engineering, JSCE, No.724(I-62), pp.49-67, 2003. (in Japanese)